Narrow-Linewidth Homogeneous Optical Emitters in Diamond Nanostructures via Silicon Ion Implantation

Coherent optical emitters in diamond nanostructures via ion implantation

Ruffin E. Evans,[1,*] Alp Sipahigil,[1,*] Denis D. Sukachev,[1,2] Alexander S. Zibrov,[1] and Mikhail D. Lukin[1,†]

[1] *Department of Physics, Harvard University, 17 Oxford St., Cambridge, MA 02138*

[2] *Russian Quantum Center, Business-center "Ural", 100A Novaya St., Skolkovo, Moscow 143025*

(Dated: December 16, 2015)

The negatively-charged silicon-vacancy (SiV^-) center in diamond is a bright source of indistinguishable single photons and a useful resource in quantum information protocols. Until now, SiV^- centers with narrow optical linewidths and small inhomogeneous distributions of SiV^- transition frequencies have only been reported in samples doped with silicon during diamond growth. We present a technique for producing implanted SiV^- centers with nearly lifetime-limited optical linewidths and a small inhomogeneous distribution. These properties persist after nanofabrication, paving the way for incorporation of high-quality SiV^- centers into nanophotonic devices.

PACS numbers: 78.55.Ap, 81.05.Cy, 81.07.Gf, 42.50.Ex
Keywords: Silicon-Vacancy; ion implantation; diamond; photonics; quantum optics

I. INTRODUCTION

Coherent emitters of indistinguishable single photons are a basic ingredient in many quantum information systems[1]. Atom-like emitters in the solid state are a particularly appealing platform for practical quantum information because they can be scalably integrated into nanophotonic devices. However, no single solid-state system has yet combined high brightness of narrowband emission and a low inhomogeneous distribution of photon frequencies from separate emitters (indistinguishability) with ease of incorporation into nanophotonic structures on demand. For example, optically active semiconductor quantum dots can be bright and integrable into nanostructures, but have a large inhomogeneous distribution[2]. Nitrogen-vacancy (NV^-) centers in bulk diamond[3] are bright and photostable, with a moderate inhomogeneous distribution that allows straightforward tuning of multiple NV^- centers into resonance. These properties allow proof-of-principle demonstrations of quantum information protocols such as remote spin-spin entanglement generation[4, 5] and quantum teleportation[6]. Further progress towards developing NV^- based quantum devices has been hindered by low indistinguishable photon generation rates associated with the weak NV^- zero-phonon line, a challenge that could be addressed by integrating NV^- centers into nanophotonic structures. However, the optical transition frequencies of NV^- centers are very sensitive to their local environment[7, 8], making integration of spectrally stable emitters into nanophotonic structures a major challenge[9].

The negatively charged silicon-vacancy color center in diamond (SiV^-) has shown promise in fulfilling the key criteria of high brightness[10], lifetime-limited optical linewidths[11], and a narrow inhomogeneous distribution of optical transition frequencies[12]. The SiV^- (Fig. 1) has electronic states with strong dipole transitions where 70% of the emission is in the zero-phonon line (ZPL) at 737 nm[10]. The inversion symmetry of the SiV^- prevents first-order Stark shifts, suppressing spectral diffusion[11] and allowing indistinguishable photons to be generated from separate emitters without the need for tuning or extensive pre-selection of emitters[13]. When combined with a spin degree of freedom[14], the SiV^- center's bright narrowband transition, narrow inhomogeneous distribution, and spectral stability make it a promising candidate for applications in quantum optics and quantum information science.

Silicon-vacancy centers occur only rarely in natural diamond[16], and are typically introduced during CVD growth via deliberate doping with silane[17, 18] or via silicon contamination[11, 12, 19–21]. While these techniques typically result in a narrow inhomogeneous distribution of SiV^- fluorescence wavelengths, these samples have a number of disadvantages. For example, the concentration of SiV^- centers can be difficult to control and localization of SiV^- centers in three dimensions is impossible.

Ion implantation offers a promising solution to these problems. By controlling the energy, quantity, and isotopic purity of the source ions, the depth, concentration, and isotope of the resulting implanted ions can be controlled. Ion implantation is widely commercially available. Targeted ion

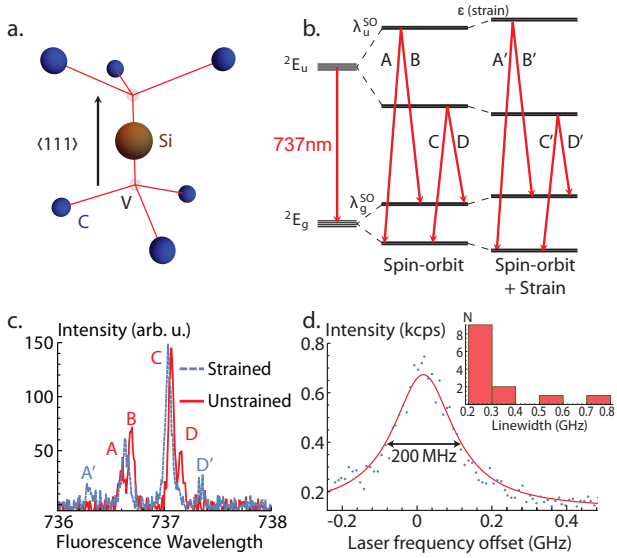

FIG. 1. Properties of the SiV^- center. **a.** Atomic structure of the SiV center. The V-Si-V axis lies along the ⟨111⟩ lattice direction. The SiV^- has D_{3d} symmetry. **b.** Level structure of the SiV^- center. The SiV^- is a single-hole system with double orbital and spin degeneracy. This degeneracy is partially lifted by spin-orbit coupling ($\lambda_g^{SO} = 47\,\text{GHz}$ and $\lambda_u^{SO} = 260\,\text{GHz}$[11, 15]). Lattice strain increases the splitting between these spin-orbit levels, shifting the transition frequencies. **c.** Fluorescence spectra of the ZPLs of single SiV^- centers in high-strain (blue, dashed) and low-strain (red) environments at 9–15 K. Transitions B and C are less sensitive to strain compared with transitions A and D because the ground and excited states shift in the same (opposite) directions for transitions B and C (A and D)[12]. **d.** Linewidth (FWHM) of representative implanted SiV^- in bulk (unstructured) diamond measured by PLE spectroscopy (blue points: data; red line: Lorentzian fit). Inset: histogram of emitter linewidths in bulk diamond. Almost all emitters have a linewidth within a factor of three of the lifetime limit (94 MHz).

implantation using a focused silicon ion beam is also possible, allowing for placement of silicon defects in all three dimensions with precision on the scale of tens of nanometers[22]. Despite the advantages of ion implantation, there have been conflicting results[15, 22, 23] on the brightness and yield of SiV^- centers produced using this method and no systematic studies of the inhomogeneous distribution of SiV^- fluorescence wavelengths. Although there has been a single report of an implanted SiV^- with a linewidth roughly 10 times the lifetime limit[24], to the best of our knowledge there has been up to now no consistent method for producing SiV^- centers with bright, narrow-linewidth emission using ion implantation. These two criteria of a low inhomogeneous distribution relative to the single-emitter linewidth and narrow single-emitter linewidth relative to the lifetime limit are essential for quantum optics applications[1, 25].

In this paper, we report the creation of SiV^- centers in diamond using ion implantation. Implantation is followed by high-temperature high-vacuum annealing to facilitate SiV^- formation and repair implantation-induced damage to the lattice. The resulting emitters have narrow optical transitions within a factor of four of the lifetime limited linewidth and a narrow inhomogeneous distribution such that the half of the emitters have transitions that lie in a 15 GHz window. Finally, we incorporate these SiV^- centers into nanostructures and demonstrate that their favorable optical properties are maintained even after fabrication.

II. THE SiV^- CENTER IN DIAMOND

The silicon-vacancy color center is a point defect in diamond wherein a silicon atom occupies an interstitial position between two vacancies (Fig. 1a)[26]. The SiV^- is a spin-$\frac{1}{2}$ system with ground (^2E_g) and excited (^2E_u) states localized to the diamond bandgap[26–28]. Both states have double spin and orbital degeneracies partially lifted by the spin-orbit interaction (Fig. 1b) which splits each quartet into two degenerate doublets. The spin-orbit splittings for the ground and excited states are 0.19 and 1.08 meV (47 and 260 GHz), respectively (Fig. 1c)[15, 27]. All transitions between the ground and excited states are dipole-allowed with a ZPL energy of 1.68 eV ($\lambda = 737$ nm) and an excited state lifetime of under 1.7 ns[29, 30]. These optical transitions can have linewidths (Fig. 1d) comparable to the lifetime limit of 94 MHz[11].

The SiV^- is sensitive to strain, which can further increase the splitting in the ground and excited state manifolds (Fig. 1b, last column)[14, 15]. Transitions B and C within the ZPL are relatively insensitive to strain (Fig. 1c)[12]. Transition C is between the lowest energy ground and excited states which are also isolated from the phonon bath at low temperatures[29]. This transition is therefore the most suitable for applications in quantum information science.

III. CREATING SiV^- CENTERS WITH ION IMPLANTATION

We create SiV^- centers using the following procedure[30]: First, we begin with a polished CVD diamond (Element Six Inc., $[N]_S^0 < 5\,\text{ppb}$, {100} oriented top face). Previous work suggests that mechanical polishing produces a strained and damaged layer close to the surface that results in reduced mechanical stability of nanofabricated structures[31, 32]. We reduce this damage by removing $5\,\mu\text{m}$ of diamond through reactive ion etching, producing a smooth (under 1 nm RMS roughness) surface. An otherwise identical control sample was also put through the same implantation procedure but without this pre-etching step. We then implant $^{29}Si^+$ ions (Innovion Corporation) at a dose of $10^{10}\,\text{ions/cm}^2$ and an energy of 150 keV resulting in an estimated depth of $100 \pm 20\,\text{nm}$[30, 33].

After implantation, we perform two high-temperature high-vacuum ($\lesssim 10^{-6}\,\text{Torr}$) anneals with dwell times of eight hours at 800 °C (where vacancies are mobile[34–36]) and, for the second anneal, two hours at 1100 °C (where divacancies and other defects can also anneal out[37, 38]). This annealing procedure, inspired by previous work with SiV^-[20, 39] and NV^-[31, 37, 40, 41] centers, both aids in the formation of SiV^- centers and also helps remove damage to the crystal lattice, reducing local strain. The residual graphitic carbon produced during these high-temperature anneals was then removed with an oxidative acid clean (boiling 1 : 1 : 1 perchloric : nitric : sulfuric acid)[42].

IV. RESULTS AND DISCUSSION

A. SiV^- centers in bulk diamond

We confirm that the SiV^- centers exhibit narrow-linewidth optical transitions by performing photoluminescence excitation (PLE) spectroscopy after 1100 °C annealing. In this experiment, we scan the frequency of a resonant laser (New Focus Velocity, linewidth $\Delta f \lesssim 25\,\text{MHz}$ over the course of the experiment) across transition C and monitor the fluorescence on the phonon-sideband (PSB). We integrate over several scans to reconstruct the time-averaged shape and position of the SiV^- ZPL (Fig. 1d). We perform these measurements at a sample stage temperature of 3.7 K to avoid phonon-induced broadening of the optical transition[29]. We find that SiV^- centers in bulk diamond have narrow optical transitions with linewidths of $\Gamma/2\pi = 320 \pm 180\,\text{MHz}$ (mean and standard deviation for N = 13 emitters). Almost all SiV^- centers have a linewidth within a factor of three of the lifetime limit (Fig. 1d, inset).

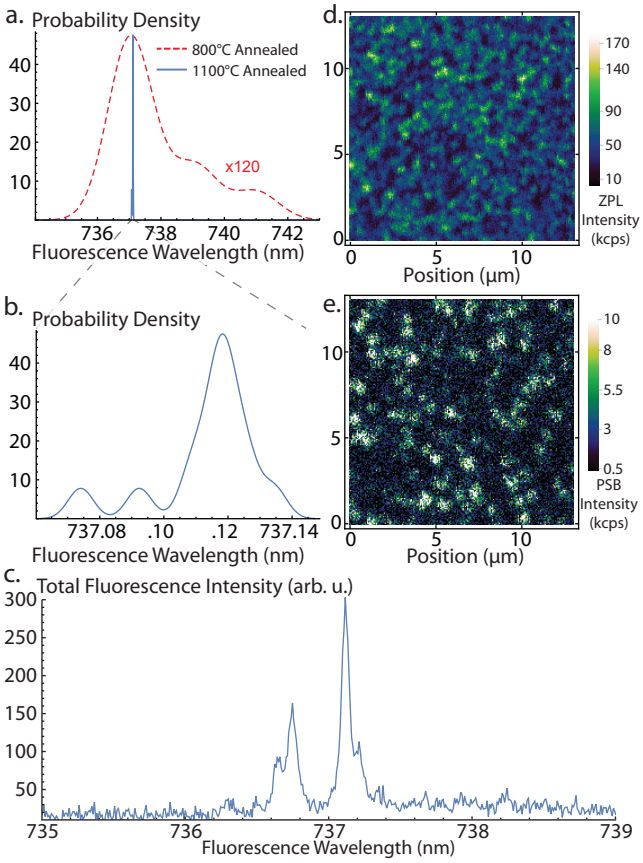

FIG. 2. Inhomogeneous distribution of fluorescence wavelengths of implanted SiV^- transitions. **a.** Kernel density estimation of distribution of bulk SiV^- wavelengths after 800 °C (N = 19, red dashed curve) and 1100 °C (N = 13, blue solid curve) annealing. The distribution narrows from 3–4 nm (800 °C anneal) to 0.03 nm (15 GHz, 1100 °C anneal). **b.** Zoomed-in distribution (transition C) after 1100 °C annealing. Note the smaller wavelength range on the horizontal axis. **c.** Sum of spectra for different SiV^- centers after 1100 °C annealing. The SiV^- fine structure is clearly present, demonstrating that the inhomogeneous distribution is small. **d**, **e.** Spatial map of collected fluorescence (thousands of counts per second) over a region of bulk diamond exciting off (d) and on (e) resonance. By comparing the densities of emitters, we estimate that $30 \pm 15\%$ of the emitters are nearly resonant. These measurements were taken at 9–15 K.

As defined here, these linewidths include the effects of phonon broadening and all spectral diffusion that happens at any timescale during the course of the experiment (4–15 minutes).

We characterize the inhomogeneous distribution of the implanted SiV^- fluorescence wavelengths after each annealing step via photoluminescence spectroscopy with a high-resolution spectrometer (Horiba iHR550, 0.025 nm resolution). We perform these measurements at 9–15 K. After annealing at 800 °C, the observed distribution is broad, with about half of the emitter transition wavelengths lying within a 3–4 nm range (Fig. 2a, red dashed curve). Transition C was used where unambiguous identification was possible; otherwise, the brightest transition (which should correspond to transition C[11, 12]) was used[30]. After the 1100 °C anneal, the distribution becomes more than 100 times narrower, with about half of the 13 measured emitters (transition C) now lying in a 0.03 nm (15 GHz) window (Fig. 2a and 2b, blue solid curves). In both cases, we focus on transition C because it is the brightest transition and relatively insensitive to strain[12] and phononic decoherence[29]. The other transitions are also much more narrowly distributed after 1100 °C annealing. In Fig. 2c, we plot a composite spectrum constructed by summing over all of the normalized 13 SiV^- spectra taken after 1100 °C annealing. This composite spectrum is very similar to the spectrum of a single unstrained SiV^- center (Fig. 1c) and shows the expected fine-structure splitting, demonstrating that the inhomogeneous distribution of SiV^- transition wavelengths is small compared to the fine-structure splitting. This result is comparable to reported inhomogeneous distributions reported for SiV^- centers created during CVD growth[11–13, 15]. It is possible that even higher temperature annealing could further reduce this inhomogeneous distribution[20, 41].

To estimate the yield of conversion from implanted Si^+ ions to SiV^- centers, we perform scanning confocal microscopy (Fig. 2d). Exciting with several milliwatts of off-resonant light (700 nm) gives around 10^5 counts per second (cps) in a single spatial mode from a single SiV^- in a 20 nm spectral range around the ZPL[30]. We analyze a series of these images and estimate our SiV^- creation yield after 800 °C annealing to be 0.5–1%. There was no clear difference in the yield after performing the 1100 °C anneal. Furthermore, the yield in the sample that was not pre-etched was significantly higher (2–3%). The observations that higher-temperature annealing did not increase the yield and that the sample with greater surface damage had a larger yield both support the model that SiV^- formation is limited by the presence and diffusion of nearby vacancies[38, 39]. This yield could be increased by electron irradiating the sample to create a higher vacancy density in a controllable way[18, 37, 39].

To visualize the density of nearly resonant SiV^- centers, we resonantly excited the SiV^- centers with a Rabi frequency of several GHz using a home-built external-cavity diode laser[30] tuned to the center of the inhomogeneous distribution. We scan spatially over the sample and collect fluorescence on the phonon side-band (PSB). The resulting image taken in the same region of the sample (Fig. 2e) has about a factor of three fewer emitters compared to the image taken with off-resonant excitation (N∼100 vs. ∼340); roughly 30% of the emitters are near-resonant.

B. SiV^- centers in nanostructures

One major advantage of building quantum devices with solid-state emitters rather than trapped atoms or ions is that solid state systems are typically more easily integrated into nanofabricated electrical and optical structures[43, 44]. The scalability of these systems is important for practical realization of even simple quantum optical devices[45]. Unfortunately, many solid-state systems suffer serious deterioration in their properties when incorporated into nanostructures. For example, the large permanent electric dipole of NV^- centers in diamond causes coupling of the NV^- to nearby electric field noise, shifting its optical transition frequency as a function of time. The SiV^- is immune to this spectral diffusion to first order because of its inversion symmetry[13] and is therefore an ideal candidate for integration into diamond nanophotonic structures. Motivated by these considerations, we fabricated an array of diamond nanophotonic waveguides (Fig. 3a) on the pre-etched sample characterized above using previously reported methods[30, 32, 46]. Each waveguide (Fig. 3a, inset) is 23 μm long with approximately equilateral-triangle cross sections of side length 300–500 nm. After fabrication, we again performed the same 1100 °C annealing and acid cleaning procedure. Many SiV^- centers are visible in a fluorescence image of the final structures (Fig. 3b).

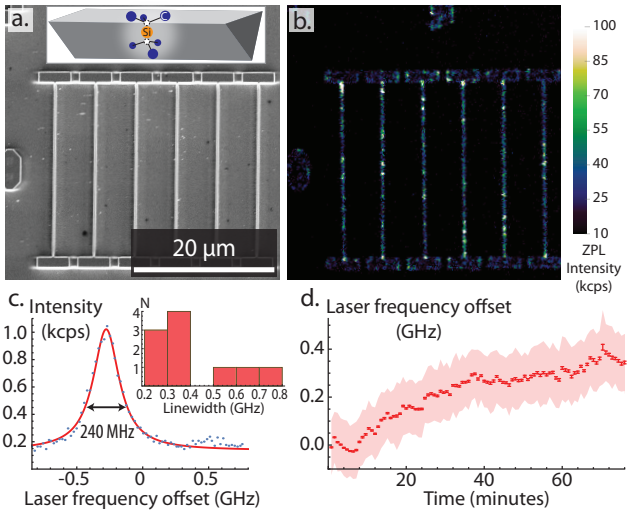

FIG. 3. SiV^- centers in nanostructures. **a.** Scanning electron micrograph of six nanobeam waveguides. Inset: schematic of a triangular diamond nanobeam containing an SiV^- center. **b.** Spatial map of ZPL fluorescence collected by scanning confocal microscopy with off-resonant excitation. Multiple bright SiV^- centers are visible in each waveguide. **c.** Linewidth of representative implanted SiV^- inside a nano-waveguide measured by PLE spectroscopy (blue points: data; red line: Lorentzian fit). Inset: histogram of emitter linewidths in nanostructures. Most emitters have linewidths within a factor of four of the lifetime limit. **d.** Spectral diffusion of the emitter measured in part c. The total spectral diffusion is under 400 MHz even after more than an hour of continuous measurement. Error bars are statistical error on the fitted center position. The lighter outline is the FWHM of the fitted Lorentzian at each time point.

To characterize the coherence properties of SiV^- centers in nanostructures, we again perform PLE spectroscopy. SiV^- centers in nanostructures have narrow transitions with a full-width at half-maximum (FWHM) of $\Gamma_n/2\pi = 410 \pm 160$ MHz (mean and standard deviation for $N = 10$ emitters; see Fig. 3c inset for linewidth histogram), only a factor of 4.4 greater than the lifetime limited linewidth $\gamma/2\pi = 94$ MHz. The linewidths measured in nanostructures are comparable to those measured in bulk (unstructured) diamond ($\Gamma_b/2\pi = 320 \pm 180$ MHz). The ratios Γ_n/γ and Γ_b/γ are much lower than the values for NV^- centers, where the current state of the art for typical implanted NV^- centers in nanostructures[9] and in bulk[31] is $\Gamma_n/\gamma \gtrsim 100$–$200$ and $\Gamma_b/\gamma \gtrsim 10$ ($\gamma/2\pi = 13$ MHz for NV^- centers). By extracting the center wavelength of each individual scan, we also determine the rate of fluctuation of the ZPL position and therefore quantify spectral diffusion (Fig. 3d). Optical transition frequencies in SiV^- centers are stable throughout the course of our experiment, with spectral diffusion on the order of the total optical linewidth even after more than an hour. Characterizing the inhomogeneous distribution of SiV^- centers in nanostructures is challenging because off-resonant excitation leads to strong background fluorescence, making exhaustive identification of all SiV^- centers in a given region difficult. Nevertheless, it is easy to find multiple SiV^- centers in nanostructures at nearly the same resonance frequency: to find the above ten emitters, we scanned the laser frequency over only a 20 GHz range.

The residual broadening of the optical transition can result from a combination of second-order Stark shifts and phonon broadening. The presence of a strong static electric field would result in an induced dipole that linearly couples to charge fluctuations, accounting for the slow diffusion. Finally, we expect that up to 50 MHz of additional broadening could arise from the hyperfine interaction[47] present due to our choice of ^{29}Si ions. Determining the precise mechanisms limiting SiV^- linewidths is an important topic of future study.

To conclude, we have presented bright optical emission from implanted SiV^- centers with a narrow inhomogeneous distribution of SiV^- optical transition wavelengths and nearly lifetime-limited optical linewidths. These properties persist after nanofabrication, making the SiV^- center uniquely suited for integration into quantum nanophotonic devices[48, 49]. Recent advances in diamond fabrication technology[32, 50, 51] suggest the tantalizing possibility of scalably integrating these high-quality implanted SiV^- centers into nanowire single photon sources[52] or nanocavities[53, 54]. Furthermore, combining our processing procedure with targeted implantation of silicon using a focused ion beam[22] could significantly improve photonic device yields and reproducibility by deterministically positioning individual SiV^- centers in all three dimensions. Our work, combined with the promise of these future advances, could make the SiV^- center a new workhorse in solid-state quantum optics.

We thank D. J. Twitchen and M. Markham from Element Six Inc. for providing the electronic grade diamond samples, A. Sushkov and S. Meesala for help with annealing, and N. P. de Leon and K. De Greve for help with etching and sample processing. We also thank Y. Chu, B. J. Shields, K. D. Jahnke,

L. J. Rogers, and F. Jelezko for discussions and valuable insight. M. L. Goldman and C. T. Nguyen helped develop some of the software used in the experiment. M. K. Bhaskar contributed to figure design.

Financial support was provided by the NSF, the Center for Ultracold Atoms, the Air Force Office of Scientific Research MURI "Multifunctional Light-Matter Interfaces based on Neutral Atoms & Solids", the DARPA QuINESS program, and the ARL. R. E. was supported in part by the NSF Graduate Research Fellowship Program. This work was performed in part at the Center for Nanoscale Systems (CNS) of Harvard University which is supported under NSF award ECS-0335765.

* These authors contributed equally.
† lukin@physics.harvard.edu

[1] J. L. O'Brien, A. Furusawa, and J. Vučković, Nat. Photonics **3**, 687 (2009).
[2] P. Lodahl, S. Mahmoodian, and S. Stobbe, Rev. Mod. Phys. **87**, 347 (2015).
[3] M. W. Doherty, N. B. Manson, P. Delaney, F. Jelezko, J. Wrachtrup, and L. C. Hollenberg, Phys. Rep. **528**, 1 (2013).
[4] H. Bernien, B. Hensen, W. Pfaff, G. Koolstra, M. S. Blok, L. Robledo, T. H. Taminiau, M. Markham, D. J. Twitchen, L. Childress, and R. Hanson, Nature **497**, 86 (2013).
[5] B. Hensen, H. Bernien, A. Dréau, A. Reiserer, N. Kalb, M. Blok, J. Ruitenberg, R. Vermeulen, R. Schouten, C. Abellán, *et al.*, Nature **526**, 682 (2015).
[6] W. Pfaff, B. Hensen, H. Bernien, S. van Dam, M. Blok, T. Taminiau, M. Tiggelman, R. Schouten, M. Markham, D. J. Twitchen, *et al.*, Science **345**, 532 (2014).
[7] P. Tamarat, T. Gaebel, J. Rabeau, M. Khan, A. Greentree, H. Wilson, L. Hollenberg, S. Prawer, P. Hemmer, F. Jelezko, *et al.*, Phys. Rev. Lett. **97**, 083002 (2006).
[8] P. Siyushev, H. Pinto, M. Vörös, A. Gali, F. Jelezko, and J. Wrachtrup, Phys. Rev. Lett. **110**, 167402 (2013).
[9] A. Faraon, C. Santori, Z. Huang, V. M. Acosta, and R. G. Beausoleil, Phys. Rev. Lett. **109**, 033604 (2012).
[10] E. Neu, D. Steinmetz, J. Riedrich-Möller, S. Gsell, M. Fischer, M. Schreck, and C. Becher, New J. Phys. **13**, 025012 (2011).
[11] L. J. Rogers, K. D. Jahnke, T. Teraji, L. Marseglia, C. Müller, B. Naydenov, H. Schauffert, C. Kranz, J. Isoya, L. P. McGuinness, *et al.*, Nat. Comm. **5**, 4739 (2014).
[12] H. Sternschulte, K. Thonke, R. Sauer, P. C. Münzinger, and P. Michler, Phys. Rev. B **50**, 14554 (1994).
[13] A. Sipahigil, K. D. Jahnke, L. J. Rogers, T. Teraji, J. Isoya, A. S. Zibrov, F. Jelezko, and M. D. Lukin, Phys. Rev. Lett. **113**, 113602 (2014).
[14] T. Müller, C. Hepp, B. Pingault, E. Neu, S. Gsell, M. Schreck, H. Sternschulte, D. Steinmüller-Nethl, C. Becher, and M. Atatüre, Nat. Comm. **5**, 3328 (2014).
[15] C. Hepp, T. Müller, V. Waselowski, J. N. Becker, B. Pingault, H. Sternschulte, D. Steinmüller-Nethl, A. Gali, J. R. Maze, M. Atatüre, *et al.*, Phys. Rev. Lett. **112**, 036405 (2014).
[16] C. Lo, Gems and Gemology **L**, 293 (2014).
[17] A. M. Edmonds, M. E. Newton, P. M. Martineau, D. J. Twitchen, and S. D. Williams, Phys. Rev. B **77**, 245205 (2008).
[18] U. F. S. D'Haenens-Johansson, A. M. Edmonds, B. L. Green, M. E. Newton, G. Davies, P. M. Martineau, R. U. A. Khan, and D. J. Twitchen, Phys. Rev. B **84**, 245208 (2011).
[19] E. Neu, C. Hepp, M. Hauschild, S. Gsell, M. Fischer, H. Sternschulte, D. Steinmüller-Nethl, M. Schreck, and C. Becher, New J. Phys. **15**, 043005 (2013).
[20] C. D. Clark, H. Kanda, I. Kiflawi, and G. Sittas, Phys. Rev. B **51**, 16681 (1995).
[21] J. L. Zhang, H. Ishiwata, T. M. Babinec, M. Radulaski, K. Müller, K. G. Lagoudakis, J. Dahl, R. Edgington, V. Soulière, G. Ferro, *et al.*, arXiv preprint arXiv:1509.01617 (2015).
[22] S. Tamura, G. Koike, A. Komatsubara, T. Teraji, S. Onoda, L. P. McGuinness, L. Rogers, B. Naydenov, E. Wu, L. Yan, *et al.*, Appl. Phys. Express **7**, 115201 (2014).
[23] C. Wang, C. Kurtsiefer, H. Weinfurter, and B. Burchard, J. Phys. B **39**, 37 (2006).
[24] B. Pingault, J. N. Becker, C. H. H. Schulte, C. Arend, C. Hepp, T. Godde, A. I. Tartakovskii, M. Markham, C. Becher, and M. Atatüre, Phys. Rev. Lett. **113**, 263601 (2014).
[25] I. Aharonovich, S. Castelletto, D. Simpson, C. Su, A. Greentree, and S. Prawer, Rep. Prog. Phys. **74**, 076501 (2011).
[26] J. P. Goss, R. Jones, S. J. Breuer, P. R. Briddon, and S. Öberg, Phys. Rev. Lett. **77**, 3041 (1996).
[27] L. J. Rogers, K. D. Jahnke, M. W. Doherty, A. Dietrich, L. P. McGuinness, C. Müller, T. Teraji, H. Sumiya, J. Isoya, N. B. Manson, *et al.*, Phys. Rev. B **89**, 235101 (2014).
[28] A. Gali and J. R. Maze, Phys. Rev. B **88**, 235205 (2013).
[29] K. D. Jahnke, A. Sipahigil, J. M. Binder, M. W. Doherty, M. Metsch, L. J. Rogers, N. B. Manson, M. D. Lukin, and F. Jelezko, New J. Phys. **17**, 043011 (2015).
[30] See Supplemental Material, available as an ancillary file on the arXiv, for additional experimental infor-

mation.
[31] Y. Chu, N. P. de Leon, B. J. Shields, B. Hausmann, R. Evans, E. Togan, M. J. Burek, M. Markham, A. Stacey, A. S. Zibrov, A. Yacoby, D. J. Twitchen, M. Lončar, H. Park, P. Maletinsky, and M. D. Lukin, Nano Lett. **14**, 1982 (2014).
[32] M. J. Burek, N. P. de Leon, B. J. Shields, B. J. Hausmann, Y. Chu, Q. Quan, A. S. Zibrov, H. Park, M. D. Lukin, and M. Lončar, Nano Lett. **12**, 6084 (2012).
[33] J. F. Ziegler, M. D. Ziegler, and J. P. Biersack, Nucl. Instr. Meth. Phys. Res. B **268**, 1818 (2010).
[34] G. Davies, S. C. Lawson, A. T. Collins, A. Mainwood, and S. J. Sharp, Phys. Rev. B **46**, 13157 (1992).
[35] P. Deák, B. Aradi, M. Kaviani, T. Frauenheim, and A. Gali, Phys. Rev. B **89**, 075203 (2014).
[36] A. M. Zaitsev, *Optical properties of diamond: a data handbook* (Springer Science & Business Media, 2001).
[37] V. Acosta, E. Bauch, M. Ledbetter, C. Santori, K.-M. Fu, P. Barclay, R. Beausoleil, H. Linget, J. Roch, F. Treussart, *et al.*, Phys. Rev. B **80**, 115202 (2009).
[38] T. Yamamoto, T. Umeda, K. Watanabe, S. Onoda, M. Markham, D. J. Twitchen, B. Naydenov, L. McGuinness, T. Teraji, S. Koizumi, *et al.*, Phys. Rev. B **88**, 075206 (2013).
[39] C. D. Clark and C. Dickerson, Surf. Coat. Tech. **47**, 336 (1991).
[40] S. Pezzagna, B. Naydenov, F. Jelezko, J. Wrachtrup, and J. Meijer, New Journal of Physics **12**, 065017 (2010).
[41] J. Orwa, C. Santori, K. Fu, B. Gibson, D. Simpson, I. Aharonovich, A. Stacey, A. Cimmino, P. Balog, M. Markham, *et al.*, J. Appl. Phys. **109**, 083530 (2011).
[42] M. Hauf, B. Grotz, B. Naydenov, M. Dankerl, S. Pezzagna, J. Meijer, F. Jelezko, J. Wrachtrup, M. Stutzmann, F. Reinhard, *et al.*, Phys. Rev. B **83**, 081304 (2011).
[43] T. D. Ladd, F. Jelezko, R. Laflamme, Y. Nakamura, C. Monroe, and J. L. O'Brien, Nature **464**, 45 (2010).
[44] K. J. Vahala, Nature **424**, 839 (2003).
[45] Y. Li, P. C. Humphreys, G. J. Mendoza, and S. C. Benjamin, Phys. Rev. X **5**, 041007 (2015).
[46] B. J. Hausmann, B. J. Shields, Q. Quan, Y. Chu, N. P. de Leon, R. Evans, M. J. Burek, A. S. Zibrov, M. Markham, D. J. Twitchen, *et al.*, Nano Lett. **13**, 5791 (2013).
[47] L. J. Rogers, K. D. Jahnke, M. H. Metsch, A. Sipahigil, J. M. Binder, T. Teraji, H. Sumiya, J. Isoya, M. D. Lukin, P. Hemmer, *et al.*, Phys. Rev. Lett. **113**, 263602 (2014).
[48] I. Aharonovich, A. D. Greentree, and S. Prawer, Nat. Photonics **5**, 397 (2011).
[49] B. J. Hausmann, B. Shields, Q. Quan, P. Maletinsky, M. McCutcheon, J. T. Choy, T. M. Babinec, A. Kubanek, A. Yacoby, M. D. Lukin, *et al.*, Nano Lett. **12**, 1578 (2012).
[50] J. Riedrich-Möller, L. Kipfstuhl, C. Hepp, E. Neu, C. Pauly, F. Mücklich, A. Baur, M. Wandt, S. Wolff, M. Fischer, *et al.*, Nat. Nanotech. **7**, 69 (2012).
[51] M. J. Burek, Y. Chu, M. S. Liddy, P. Patel, J. Rochman, S. Meesala, W. Hong, Q. Quan, M. D. Lukin, and M. Lončar, Nat. Comm. **5**, 5718 (2014).
[52] T. M. Babinec, B. J. Hausmann, M. Khan, Y. Zhang, J. R. Maze, P. R. Hemmer, and M. Lončar, Nat. Nanotech. **5**, 195 (2010).
[53] J. C. Lee, I. Aharonovich, A. P. Magyar, F. Rol, and E. L. Hu, Opt. Express **20**, 8891 (2012).
[54] J. Riedrich-Möller, C. Arend, C. Pauly, F. Mucklich, M. Fischer, S. Gsell, M. Schreck, and C. Becher, Nano Lett. **14**, 5281 (2014).